Available online at www.sciencedirect.com
ScienceDirect
Journal of Solid State Chemistry 180 (2007) 1664–1671
JOURNAL OF SOLID STATE CHEMISTRY
www.elsevier.com/locate/jssc

Two-dimensional layer architecture assembled by Keggin polyoxotungstate, Cu(II)–EDTA complex and sodium linker: Synthesis, crystal structures, and magnetic properties

Hong Liu[a,b], Lin Xu[a,*], Guang-Gang Gao[a], Feng-Yan Li[a], Yan-Yan Yang[a], Zhi-Kui Li[a], Yu Sun[a]

[a]*Key Laboratory of Polyoxometalates Science of Ministry of Education, College of Chemistry, Northeast Normal University, Changchun 130024, PR China*
[b]*College of Chemistry and Medicine, Jiamusi University, Jiamusi 154007, PR China*

Received 24 November 2006; received in revised form 4 March 2007; accepted 11 March 2007
Available online 16 March 2007

Abstract

Reaction of Keggin polyoxotungstate with copper(II)–EDTA (EDTA = ethylenediamine tetraacetate) complex under mild conditions led to the formation of hybrid inorganic–organic compounds $Na_4(OH)[(Cu_2EDTA)PW_{12}O_{40}]\cdot 17H_2O$ (1) and $Na_4[(Cu_2EDTA)SiW_{12}O_{40}]\cdot 19H_2O$ (2). The single-crystal X-ray diffraction analyses reveal their two structural features: (1) one-dimensional chain structure consisting of Keggin polyoxotungstate and copper(II)–EDTA complex; (2) Two-dimensional layer architecture assembled by the one-dimensional chain structure and sodium linker. The results of magnetic measurements in the temperature range 300–2 K indicated the existence of ferromagnetic exchange interactions between the Cu^{II} ions for both compounds. In addition, TGA analysis, IR spectra, and electrochemical properties were also investigated to well characterize these two compounds.

Keywords: Polyoxotungstates; Copper(II)–EDTA; Crystal structures; Magnetic properties

1. Introduction

Polyoxometalates (POMs) have attracted considerable attention because of their surprising electronic versatility and structural diversity, that give rise to various applications in fields such as catalysis [1], medicine [2], material science [3], and photochemistry [4]. In particular, the study on functionalization of POMs has become a significant direction to develop new inorganic–organic hybrid materials with useful catalytic, optical, electronic and magnetic properties. Therefore, the recent effort has been devoted to finding the effective linker of POM building units so as to form novel one dimensional (1D) or two dimensional (2D) structures with potential applications. To date, many hybrid compounds based on vanadium and molybdenum isopolyanions or heteropolyanions have been reported, whereas the investigation incorporating polyoxotungstates and their derivatives as the inorganic component is still rare [5]. More recently, Reinoso [6] and Lisnard [7] have reported the inorganic–organic hybrids based on saturated or monosubstituted Keggin polyanions and copper(II) complexes under conventional and hydrothermal conditions, respectively. According to these results, we are interested in exploring the applicability of saturated Keggin POMs and transition-metal-EDTA (EDTA—ethylenediaminetetraacetate) cationic complexes in the preparation of new hybrid compounds. As an excellent hexadentate ligand, EDTA is broadly used in the synthesis of transitional-metal complexes. However, the hybrid inorganic-organic compounds using EDTA as organic linker remain unexplored up to now. In this paper, we report the syntheses, crystal structure, magnetic properties of two novel 1D compounds, $Na_4(OH)[Cu_2(EDTA)PW_{12}O_{40}]\cdot 17H_2O$ (**1**) and $Na_4[Cu_2(EDTA)SiW_{12}O_{40}]\cdot 19H_2O$ (**2**), assembled by the linker of copper(II)–EDTA complex with Keggin-type polyoxotungstate. This result suggests that Keggin-POM-based coordination polymers with

*Corresponding author. Fax: +86 0431 85099668.
E-mail address: linxu@nenu.edu.cn (L. Xu).

0022-4596/$ - see front matter © 2007 Elsevier Inc. All rights reserved.
doi:10.1016/j.jssc.2007.03.011

unprecedented topology and attractive properties could be obtained by rationally selecting organic linker [8].

2. Experimental

2.1. General procedures

All reagents were purchased and used without further purification. Elemental analyses (W, Cu, P, Si, Na) were determined by a Leeman inductively coupled plasma (ICP) spectrometer. The infrared spectrum was recorded with an Alpha Centaur FT/IR spectrometer with a KBr pellet in the 4000–400 cm^{-1} region. The thermal gravimetric analysis (TGA) is carried out under N_2 at a rate of 5 °C/min in the range 20–800 °C. Electronic spectra ware performed in aqueous solutions within a range of $\lambda = 190$–800 nm using an ATI Uncial-UV–Visible Vision Software V3.20. Variable-temperature magnetic susceptibility was performed with an Oxford Maglab 2000 System or a Quantum Design MPMS XL-5 SQUID system. Electrochemical experiments were performed with a CHI 660 electrochemical workstation for control of the electrochemical measurements and for data collection. A conventional three-electrode system was used to investigate the cyclic voltammetric behaviors. The glass carbon electrode was used as a working electrode; Ag/AgCl as a reference electrode; Pt coil as a counter electrode, and the 0.2 mol/L Na_2SO_4/H_2SO_4 solution (pH = 3) was used as electrolyte.

2.2. Syntheses of compounds

Synthesis of **1**: $Na_2WO_4 \cdot 2H_2O$ (5.000 g, 15.2 mmol) was dissolved in 20 mL deionized water and the solution was heated to 90 °C for about 10 min. Then H_3PO_4 (0.169 g, 1.7 mmol) dissolved in 3 mL 6 mol/L HCl solution and $Cu(Ac)_2 \cdot H_2O$ (1.572 g, 7.9 mmol) dissolved in 10 mL saturated NaCl solution were added to the heated solution. The pH value was adjusted to 3.33 and the mixture was kept at 90 °C for about 1 h. At last disodium EDTA (0.20 g, 1.38 mmol) was added and stirring continued for about 1 h. The solution was cooled to room temperature and filtered. The transparent blue-green filtrate was retained in room temperature for 16 days to form blue crystals. A rectangular parallelepiped (0.60 mm × 0.30 mm × 0.25 mm) crystal was obtained suitable for X-ray diffraction determination. The yield was 54% (based on W). anal. calcd. (found) for $C_{10}H_{47}Cu_2N_2Na_4O_{66}PW_{12}$ (%): Cu, 3.43 (3.51); P, 0.84 (0.89); W, 59.49 (60.03); Na, 2.48 (2.53). IR (KBr pellet, cm^{-1}): 3745 (w), 3450 (s), 2952 (m), 2881 (m), 2362 (s), 1633 (s), 1383 (w), 1106 (w), 1060 (s), 960 (s), 886 (w), 811 (s), 747 (m), 691 (m).

2 was synthesized by a similar procedure except that H_3PO_4 was replaced by $Na_2SiO_3 \cdot 9H_2O$ (0.432 g, 1.52 mmol). A rectangular parallelepiped (0.50 mm × 0.20 mm × 0.15 mm) crystal of **2** was obtained suitable for X-ray diffraction determination. The yield was 50% (based on W). anal. calcd. (found) for $C_{10}H_{50}Cu_2N_2Na_4O_{67}SiW_{12}$ (%): Cu, 3.41 (3.53); Si, 0.75 (0.81); W, 59.24 (60.03); Na, 2.47 (2.43). IR (KBr

Table 1
Crystal data and structure refinement for **1** and **2**

Compound	**1**	**2**
Empirical formula	$C_{10}H_{47}Cu_2N_2Na_4O_{66}PW_{12}$	$C_{10}H_{50}Cu_2N_2Na_4O_{67}SiW_{12}$
Formula weight	3707.55	3723.55
Temperature	293(2) K	293(2) K
Wavelength	0.71073 Å	0.71073 Å
Crystal system, space group	triclinic, $P-1$	triclinic, $P-1$
Unit cell dimensions	$a = 11.700(2)$ Å	$a = 11.654(2)$ Å
	$b = 12.164(2)$ Å	$b = 12.148(2)$ Å
	$c = 12.689(3)$ Å	$c = 12.695(3)$ Å
	$\alpha = 67.94(3)^\circ$	$\alpha = 67.43(3)^\circ$
	$\beta = 76.89(3)^\circ$	$\beta = 77.66(3)^\circ$
	$\gamma = 85.37(3)^\circ$	$\gamma = 86.11(3)^\circ$
Volume	1629.9(6) $Å^3$	1621.1(5) $Å^3$
Z, Calculated density	2, 3.770 mg/m^3	2, 3.775 mg/m^3
$F(000)$	1647	1626
θ range for data collection	3.25–27.48°	3.43–27.48°
Limiting indices	$-13 \leqslant h \leqslant 15$, $-15 \leqslant k \leqslant 15$, $-16 \leqslant l \leqslant 16$	$-15 \leqslant h \leqslant 15$, $-15 \leqslant k \leqslant 15$, $-16 \leqslant l \leqslant 16$
Reflections collected/unique	15907/7244 [$R_{int} = 0.0687$]	14106/6532 [$R_{int} = 0.0450$]
Completeness	96.9%	97.4%
Absorption correction	Full-matrix least-squares on F^2	Full-matrix least-squares on F^2
Refinement method	7244/0/457	6532/0/445
Data/restraints/parameters Goodness-of-fit on F^2	1.025	0.999
Final R indices [$I > 2\sigma(I)$]	[a] $R_1(F_o) = 0.0710$, [b] $wR_2(F_o^2) = 0.1686$	[a] $R_1(F_o) = 0.0952$, [b] $wR_2(F_o^2) = 0.1919$
R indices (all data)	[a] $R_1(F_o) = 0.1016$, [b] $wR_2(F_o^2) = 0.1855$	[a] $R_1(F_o) = 0.1040$, [b] $wR_2(F_o^2) = 0.1970$
Largest diff. peak and hole	2.333 and −2.057e $Å^{-3}$	2.694 and −2.773e $Å^{-3}$

[a] $R_1 = (\sum|F_o| - |F_c|)/(\sum|F_c|)$.
[b] $wR_2 = \sum[w(F_o^2 - F_c^2)^2]/\sum[w(F_o^2)^2]^{1/2}$.

pellet, cm^{-1}): 3846 (w), 3745 (w), 3442 (s), 2925 (w), 2850 (m), 2362 (s), 1633 (s), 1457 (s), 1097 (m), 1014 (m), 940 (m), 886 (s), 783 (s), 580 (m), 516 (m). It should be noteworthy, when the pH value of the reaction solution extended from 3.0 to 5.0, these two crystal products were also obtained, indicating that compounds **1** and **2** could exist in a wide pH value range.

2.3. X-ray crystallography

Blue single crystals of **1** and **2** were collected on a Rigaku R-AXIS RAPID IP diffractometer with graphite monochromated Mo-$K\alpha$ radiation ($\lambda = 0.71073$ Å) at 293 K in the range of $3.25 < \theta < 27.48$ and $3.43 < \theta < 27.48$, respectively. All the structures were solved by direct methods and refined using the full-matrix least-squares method on F^2 with SHELXTL [14] crystallographic software package. The Lorentz polarization and absorption effects ware corrected for all data. Hydrogen atoms were included in the refinement using the riding model. Occupancy ratio of O27, O28, O30, and O31 atoms in **1** and O22, O24, O26, and O28 atoms in **2** are all assigned as 0.5. Selected collection parameters and other crystallographic results are summarized in Table 1. Further details of the crystal structure investigations of **1** and **2** may be obtained from the Cambridge Crystallographic Data Center with CCDC-293606 (**1**) and CCDC-293605 (**2**). These data can be obtained free of charge via ⟨www.ccdc.cam.ac.uk/data_request/cif⟩.

3. Results and discussion

3.1. Description of crystal structures

The structures of **1** and **2** display a unique 1D chains and they contain the polymeric hybrid polyanion $[Cu_2(EDTA)MW_{12}O_{40}]^{n-}$ [M = P(**1**), Si(**2**); n = 3, 4] (Fig. 1). The main structural feature of these two compounds is that the copper(II)–EDTA complex units are linked with the inorganic building blocks of the saturated Keggin polyanions (Fig. 2). The single-crystal X-ray diffraction analyses reveal that compound **1** and **2** are isostructural. The inorganic building block in the two compounds consists of a central PO_4 or SiO_4 tetrahedron (the four oxygen atoms are disordered over eight crystallographic positions and the occupancy sites are fixed as 0.5) surrounded by four vertex-sharing W_3O_{13} trimers, which result from the association of three edge-sharing $\{MO_6\}$ octahedra. The W–O distances can be sorted into three sets: W–O_t (terminal), W–$O_{b/c}$ (bridge) and W–O_a (central), which are summarized in Table 2. The metal complex building blocks are made of two copper ions bridged by an EDTA ligand and are both centrosymmetric in the two

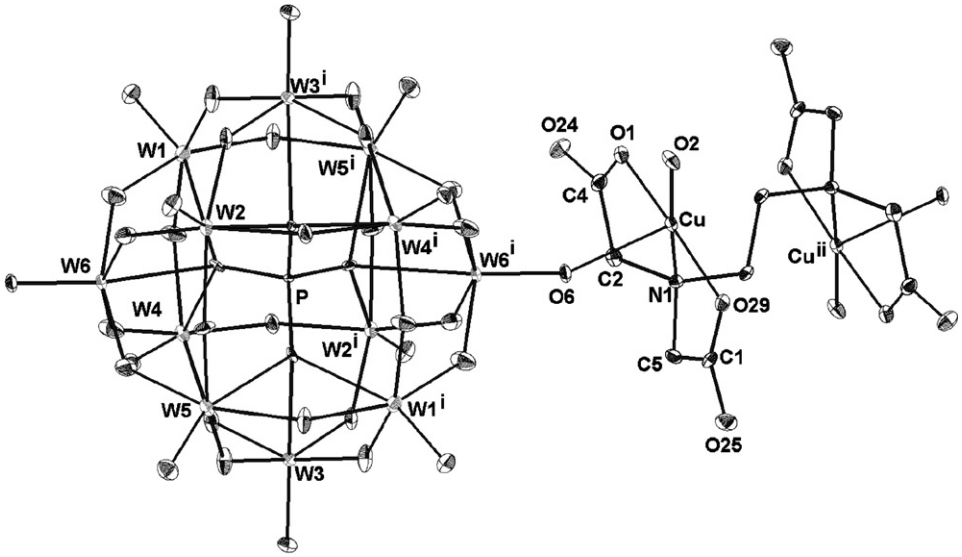

Fig. 1. Thermal ellipsoid representation (at 20% probability) of molecular structure unit of compound **1**. All the H and Na atoms and isolated water molecules are omitted. Symmetry codes: (i) $1-x$, $-y$, $1-z$; (ii) $-x$, $-y$, $-z$.

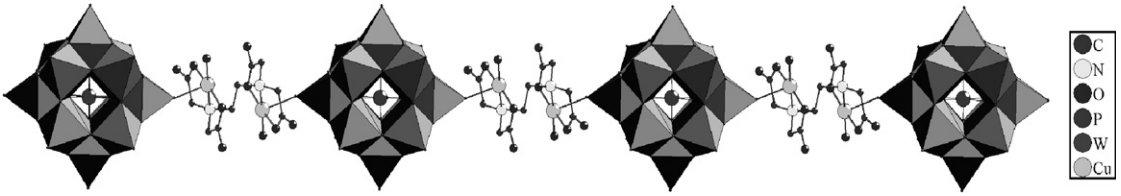

Fig. 2. A view of the one-dimensional framework of compound **1**, with ball–stick and polyhedron representation. All the H atoms are omitted for clarity.

Table 2
Selected bond lengths [Å] and angles [°] for **1** and **2**

1		**2**	
W(1)–O(12)	1.702(17)	W(2)–O(2)	1.70(2)
W(1)–O(8)#1	1.868(18)	W(2)–O(32)	1.88(4)
W(1)–O(14)	1.883(19)	W(2)–O(10)	1.90(3)
W(1)–O(33)#1	1.922(19)	W(2)–O(27)	1.91(3)
W(1)–O(10)#2	1.928(19)	W(2)–O(31)	1.94(4)
W(1)–O(28)	2.43(3)	W(2)–O(24)	2.28(4)
W(1)–O(31)	2.52(2)	W(2)–O(26)	2.31(3)
W(5)–O(7)	1.722(18)	W(4)–O(7)#1	1.73(2)
W(5)–O(16)#7	1.872(16)	W(4)–O(19)#1	1.84(5)
W(5)–O(8)	1.891(17)	W(4)–O(23)	1.86(5)
W(5)–O(13)	1.909(19)	W(4)–O(27)#1	1.91(3)
W(5)–O(26)#1	1.929(18)	W(4)–O(1)	1.93(3)
W(5)–O(27)#1	2.46(3)	W(4)–O(22)	2.29(4)
W(5)–O(31)#1	2.50(2)	W(4)–O(26)#1	2.36(3)
W(6)–O(6)	1.698(14)	W(5)–O(3)	1.734(17)
W(6)–O(26)	1.855(18)	W(5)–O(23)	1.87(5)
W(6)–O(10)	1.89(2)	W(5)–O(32)	1.86(4)
W(6)–O(19)	1.893(18)	W(5)–O(33)	1.89(3)
W(6)–O(21)	1.93(2)	W(5)–O(18)	1.91(4)
W(6)–O(28)#2	2.46(2)	W(5)–O(24)	2.27(4)
W(6)–O(27)	2.49(3)	W(5)–O(22)	2.31(4)
Cu–O(1)	1.931(15)	Cu–O(14)	1.905(19)
Cu–O(29)	1.936(15)	Cu–O(8)	1.94(2)
Cu–O(2)	1.938(16)	Cu–O(11)	1.972(17)
Cu–N(1)	1.991(17)	Cu–N	2.00(2)
Cu–O(6)	2.305(14)	Cu–O(3)	2.266(18)
O(1)–Cu–O(29)	169.1(7)	O(14)–Cu–O(8)	92.3(9)
O(1)–Cu–O(2)	91.5(7)	O(14)–Cu–O(11)	167.6(8)
O(29)–Cu–O(2)	99.3(8)	O(8)–Cu–O(11)	99.7(9)
O(1)–Cu–N(1)	85.5(7)	O(14)–Cu–N	85.2(9)
O(29)–Cu–N(1)	83.7(7)	O(8)–Cu–N	173.1(9)
O(2)–Cu–N(1)	174.5(7)	O(11)–Cu–N	82.5(8)
O(1)–Cu–O(6)	91.1(6)	O(14)–Cu–O(3)	94.1(7)
O(29)–Cu–O(6)	90.0(6)	O(8)–Cu–O(3)	90.9(8)
O(2)–Cu–O(6)	90.9(6)	O(11)–Cu–O(3)	89.0(7)
N(1)–Cu–O(6)	93.8(6)	N–Cu–O(3)	95.6(8)

1: #1 $-x+1, -y, -z$; #2 $-x+1, -y, -z+1$; #3 $-x, -y, -z+1$; #4 $-x, -y, -z$; #5 $x, y, z-1$; #6 $x-1, y, z$; #7 $x+1, y, z-1$.
2: #1 $-x+2, -y+2, -z$.

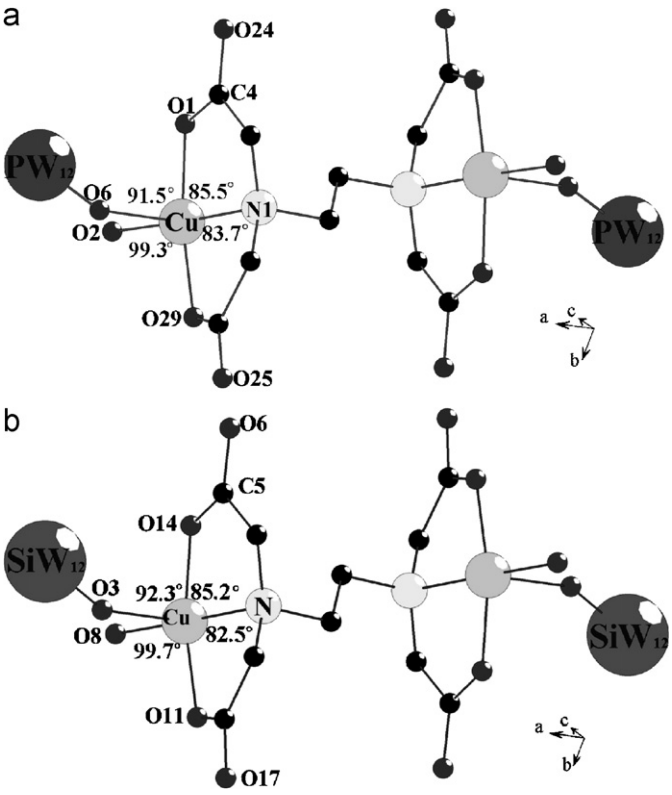

Fig. 3. Representation of the Cu-EDTA complexes: (a) **1**; (b) **2**.

compounds. Each copper ion coordinates to oxygen atoms O1 and O29 (or O14 and O11) of the carboxyl groups and one nitrogen atom. The other two sites are one water molecule and a terminal oxygen atom O2 for **1** (O8 for **2**) from the $\{WO_6\}$ unit (Fig. 3). Thus, each $\{CuO_4N\}$ group displays a five coordinate environment. Cu, N1, O1, O2, O29 in **1** and Cu, N, O14, O8, O11 in **2** are almost in the same plane with central copper ion, where the sum of O–Cu–O and N–Cu–O angles is close to 360° for two compounds (359.7° for **1** and 360.0° for **2**). The terminal oxygen atom from the Keggin polyanion can be considered as an apical ligand, with the Cu–O_t distance of 2.305 Å for **1** (and 2.266 Å for **2**), and the coordination sphere of the copper atoms can be described as an approximately square pyramids. Although these Cu–O_t distances are a little long, which may result from the Jahn–Teller effect, the interaction between dicopper complex and Keggin polyanion should be of significance for the structural stability of compounds **1** or **2**. In several previously published reports, such long Cu–O_t distances frequently appeared in the type of POM-based Cu(II) complexes [7,16]. For example, some longer Cu–O_t distances such as 2.48–2.98 Å, also play an important role in the construction of Cu(II)-complex-functionalized polyoxotungstates [7,16]. In addition, such Cu–O_t linkage between building blocks produces linear chains built of alternating POMs and copper(II)–EDTA complexes. As expected, the copper(II)–EDTA complex coordinate to neighboring two Keggin polyanions through one bridge oxygen atom to form a 1D chain $[Cu_2(EDTA)MW_{12}O_{40}]^{n-}_{\infty}$ (M = P or Si; n = 3 or 4), which is a little different from the reported copper(II)–oxalate-linked copper(II)-monosubstituted Keggin polyanions with zig-zagging-chain structure [6]. The structure of **2** is similar to **1** except that the Cu–O and Cu–N distances are a little different (Fig. 3). It is worth mentioning here that Cu–O_t distance 2.266 Å of **2** is a little shorter than that in **1** (2.305 Å). This subtle difference in the crystal structure is also confirmed by the magnetic results. Moreover, the sodium counterions were also located in the crystal structure to stabilize this network and reach charge balance. All the sodium counterions fill the space and link the neighboring chains to form 2D framework, as shown in Fig. 4. The Na–O bond lengths are in the range 2.328(2)–2.541(2) Å for **1** and 2.333(3)–2.530(4) Å for **2**. These Na–O bond lengths are comparable with some

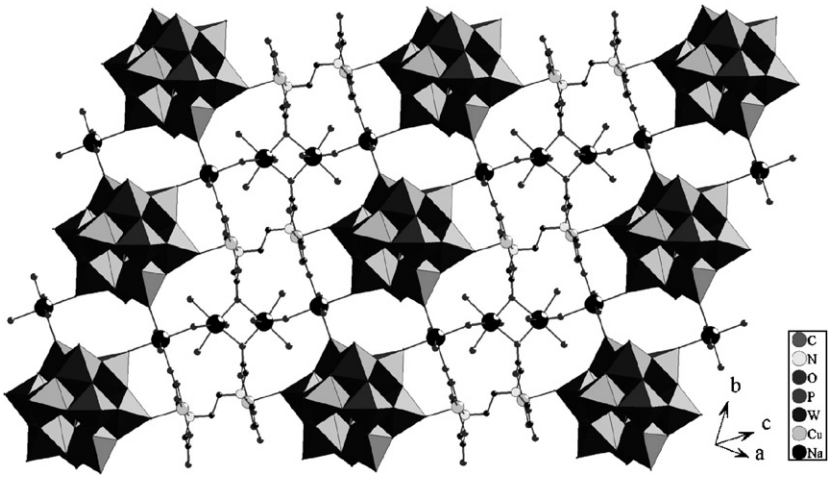

Fig. 4. A polyhedral/ball-and-stick representation of the layer structure of compound **1**. All the H and isolated water molecules are omitted.

reported analogous compounds, in which the Na–O bond lengths of 2.59–2.64 Å could exist [17,18]. Although this type of Na–O bond lengths are somewhat longer than the conventional Na–O bond length, they play a significant role in structural construction. Interestingly, in such 2D framework, the remaining oxygen atoms of the carboxyl group of EDTA further coordinate to Na^+ ions and thus all the ten potential coordinate atoms of EDTA are attributable to the formation of the 2D network. According to our knowledge, this is an unprecedented coordination environment and extends the application of EDTA as organic ligand in forming such inorganic–organic hybrids.

3.2. Cyclic voltammetry

Fig. 5 shows the electrochemical behavior for compounds **1** and **2**. In the potential range 0.5 to −0.8 V, the first (I–I′) and the second (II–II′) pairs of reversible redox peaks appear and the mean peak potentials $E_{1/2} = (E_{cp} + E_{ap})/2$ are −0.739 and −0.553 V for **1,** and −0.699 and −0.534 V for **2**. The values of peak-to-peak separations between the corresponding anodic and cathodic peaks (ΔE_p) are 41 (I–I′) and 34 mV (II–II′) for **1**, and 39 (I–I′) and II–II′ 31 mV (II–II′) for **2**; these were ascribed to two-electron redox process of W atoms, which is similar to that of the reported analogue [9]. Further, we can observe the irreversible redox process for the Cu^{2+} centers in copper(II)–EDTA complex, and the observed reduction peak potentials are −0.130 and −0.282 V for **1,** and −0.112 and −0.278 V for **2**. The pattern of such two-step reduction from Cu^{2+} to Cu^0 through Cu^+ was also similar to that of the reported analogue [10]. The above results indicate that Cu^{2+} ions are firstly reduced to Cu^+ ions in the reduced process and then they are reduced to Cu^0. When more negative potentials are applied to this system, it is observed that the occurrence of two step two-electron reduction process that is ascribed to the polyoxoanions. The possible

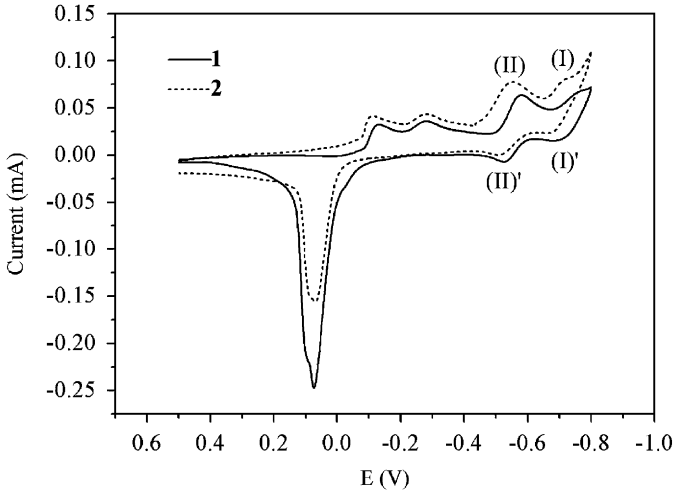

Fig. 5. Cyclic voltammograms of a 5.0×10^{-4} mol/L solution of **1** and **2** in 0.2 mol/L Na_2SO_4/H_2SO_4 electrolyte (pH = 3). The working electrode: glassy carbon; reference electrode: SCE; scan rate: 100 mV s^{-1}.

redox process is denoted here as follows [15]:

$$Cu^{2+} + e^- = Cu^+,$$

$$Cu^+ + e^- = Cu^0,$$

$$PW_{12}O_{40}^{3-}/SiW_{12}O_{40}^{4-} + 2e^- = PW_{12}O_{40}^{5-}/SiW_{12}O_{40}^{6-},$$

$$PW_{12}O_{40}^{5-}/SiW_{12}O_{40}^{6-} + 2e^- + 2H^+ = H_2PW_{12}O_{40}^{5-}/H_2SiW_{12}O_{40}^{6-}.$$

These analogue electrochemical properties are consistent with the aforementioned structures of **1** and **2** because they share a very similar chemical environment. On the other hand, it can also be concluded that the electrochemical behaviors of saturated Keggin-type heteropolytungstate anions are slightly affected by the weak coordinated copper(II) complex.

3.3. Electronic spectroscopy

The UV–Vis electronic spectra of the two compounds are displayed in Fig. 6. Keggin-type polyanion of **1** and **2** show absorption maxima at nearly the same wavelength (λ_{max}(**1**) = 257 nm; λ_{max}(**2**) = 257 nm), which are the characteristic charge transfer bands from oxygen to tungsten in the POM framework [11]. The electronic spectra in visible region exhibit a broad transition band at 783 nm for **1** and 747 nm for **2**, this broad transition band is attributed to the *d–d* electron transition in dicopper complex [12].

3.4. Thermogravimetric analysis (TGA)

TGA was performed under N_2 at a rate of 5.00 °C/min in the range 30–800 °C on compound **1** and **2** (Fig. 7). A first consecutively weight loss of 8.8% occurred between 30 and 210 °C on compound **1**, corresponding to the loss of free water molecules and coordinate water molecules (calculated 9.23%). The deviation of experimental value maybe related to the loss of water under ambient conditions. In the range 210–640 °C, consecutive two step weight losses were observed with total weight loss of 7.8% corresponding to the loss of all EDTA molecules (calculated 7.9%). For compound **2**, a first consecutively weight loss of 9.2% occurred between 30 and 206 °C, corresponding to the loss of free water molecules and coordinate water molecules (calculated 10.2%). In the range 206–610 °C, the weight losses of two steps occurred with total weight loss of 7.7%, corresponding to the loss of all EDTA molecules (calculated 7.9%).

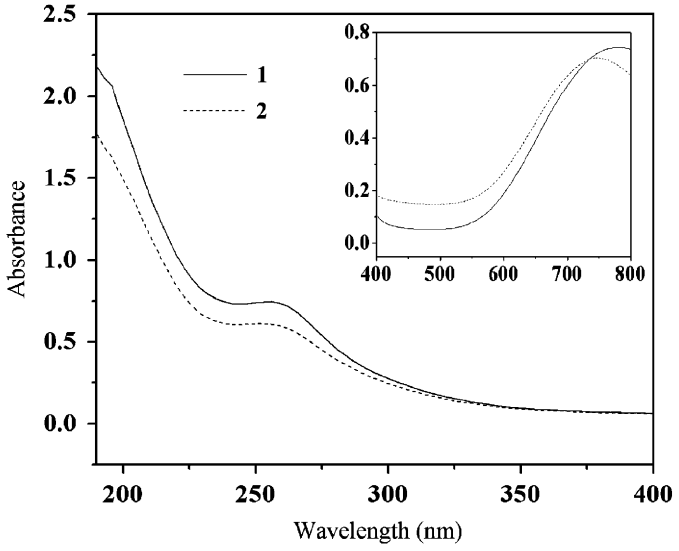

Fig. 6. UV–Vis electronic spectra in aqueous solutions for **1** and **2** within a range of 190–800 nm, 1.0×10^{-4} mol/L in ultraviolet region and 2.0×10^{-3} mol/L in the visible region.

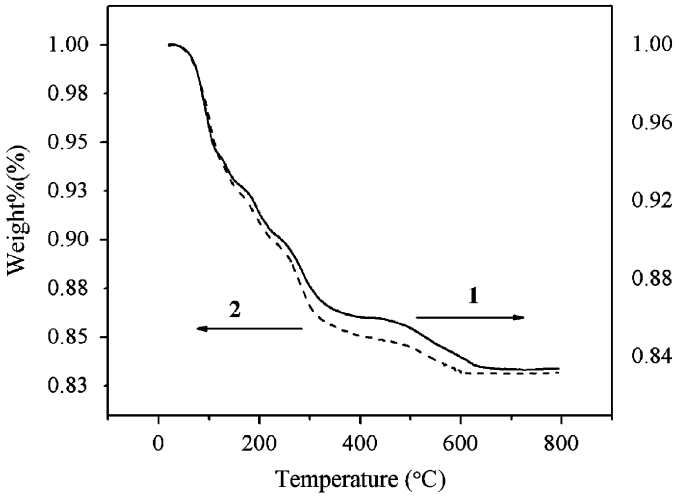

Fig. 7. TGA of **1** and **2** recorded under an N_2 atmosphere in the range 30–800 °C.

3.5. Magnetic properties

The variable–temperature magnetic susceptibility of **1** and **2** was measured under the applied magnetic field of 10 kOe in the temperature range 2–300 K. Fig. 8 shows the magnetic behavior of **1** and **2** in the forms of $\chi_m T$ vs. T curves. As shown in Fig. 8(a) for **1**, $\chi_m T$ increases from

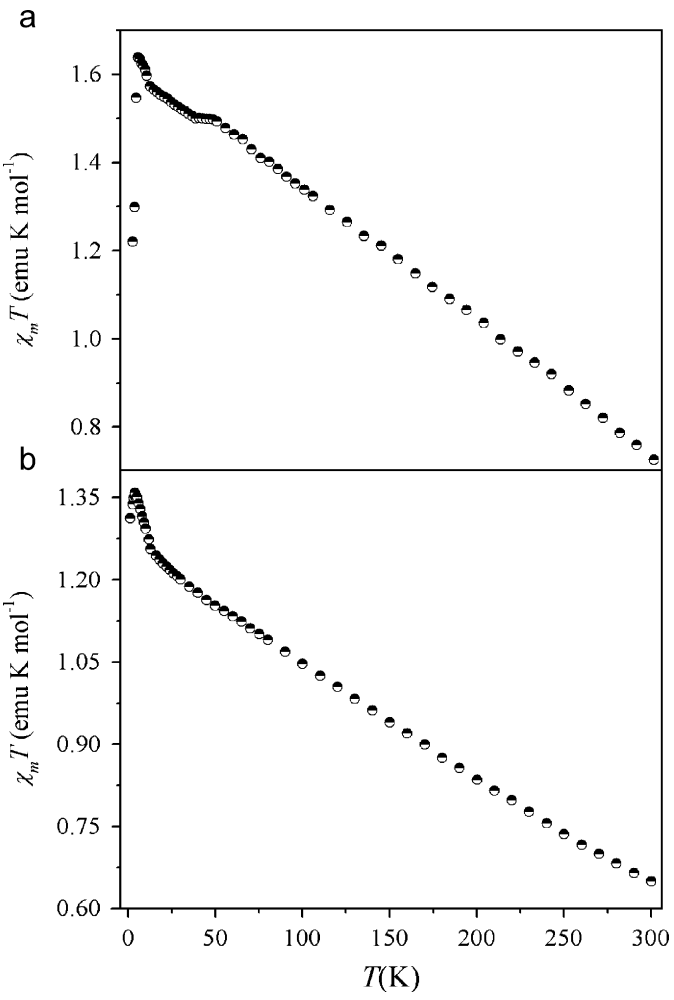

Fig. 8. Temperature dependence of $\chi_m T$ product for compounds **1** and **2** over a temperature range of 2–300 K.

$0.72\,cm^3\,K\,mol^{-1}$ at 300 K to $1.64\,cm^3\,K\,mol^{-1}$ at 5 K. The obvious increase of $\chi_m T$ value from 300 to 5 K is indicative of the occurrence of ferromagnetic interactions in **1**. Below 5 K, $\chi_m T$ decreases rapidly down to 2 K. The $\chi_m T$ value of **1** at room temperature is ca. $0.73\,cm^3\,K\,mol^{-1}$ ($2.43\,\mu_B$); this value is slightly smaller than that expected ($2.83\,\mu_B$) for the isolated two Cu(II) ions ($S = 1$; $g = 2.00$). At temperature of about 50 K, a small hump appeared in $\chi_m T$ vs. T curves for compound **1**. The appearance of a small hump, which is sporadically reported in some literature, is caused from the paramagnetic oxygen impurity in the sample. Assuming isotropic exchange, the exchange Hamiltonian is $H = -2J\boldsymbol{S}_A\boldsymbol{S}_B$ with $\boldsymbol{S}_A = \boldsymbol{S}_B = 1/2$, and the experimental magnetic susceptibility of compound **1** is actually fitted by the following Bleaney–Bowers equation [13]. Here, N is the Avogadro number, k the Boltzmann is constant, β the electronic Bohr magneton, and g the Landé tensor:

$$\chi_m = 2Ng^2\beta^2/[kT(3 + e^x)], \quad x = -J/kT. \tag{1}$$

The best fit gives magnetic coupling constant $J = 28.27\,cm^{-1}$ assuming $g = 2.26$, with agreement factor R {defined as $\sum_i[(\chi_m T)_{obs}(i) - (\chi_m T)_{calc}(i)]^2/\sum_i[(\chi_m T)_{obs}(i)]^2$} being 3.1×10^{-4}. The positive J value suggests the occurrence of an obvious ferromagnetic Cu(II)–Cu(II) interactions in **1,** being in well agreement with the $\chi_m T$ vs. T curve behavior in the temperature range of 300–5 K.

As shown in Fig. 8(b) for compound **2**, an obvious increase of $\chi_m T$ value from $0.65\,cm^3\,K\,mol^{-1}$ at 300 K to $1.36\,cm^3\,K\,mol^{-1}$ at 4 K shows the occurrence of ferromagnetic exchange interactions, as the structural feature of **2** is similar to that of **1**. In the same pattern as in **1**, below 4 K, $\chi_m T$ decreases rapidly down to 2 K. Considering a similar structure of **2** to **1**, the experimental magnetic data for compound **2** was also fitted by Eq. (1), and the best fit gives magnetic coupling constant $J = 33.15\,cm^{-1}$ assuming $g = 2.26$, with agreement factor R being 4.4×10^{-4}. In the same way, the positive J value is indicative of the occurrence of an obvious ferromagnetic Cu(II)–Cu(II) interactions in **2**. The $\chi_m T$ value of **2** at room temperature is ca. $0.65\,cm^3\,K\,mol^{-1}$ ($2.28\,\mu_B$), which is smaller than that to expected ($2.83\,\mu_B$) for the isolated two Cu(II) ions ($S = 1$; $g = 2.00$). The slight difference of the magnetic data for the two compounds may be because the Cu–O_t distance for **2** (2.266 Å) is shorter than that for **1** (2.305 Å).

In general, the long distance between the two coupled Cu(II) ions should be an unfavored condition of magnetic exchange interactions, but our repeated experimental results showed that the ferromagnetic interactions indeed occurred in **1** in the temperature range 5–300 K. Considering the structural feature of **1**, we can conclude that the layer structure arising from the linking of sodium ions is responsible for the occurrence of ferromagnetic interactions.

4. Conclusions

Under mild conditions, two novel inorganic–organic hybrid complexes based on saturated Keggin polyoxoanion and copper(II)–EDTA complex have been synthesized. This work confirms the feasibility using both the dinuclear transition metal complex of multidentate ligand and sodium ion as linkers to assemble Keggin polyanion based framework, which is an easy way for the synthesis and design of POM-based multidimensional architecture. Magnetic property research demonstrates the occurrence of ferromagnetic coupling interactions in the dicopper complexes.

Acknowledgment

The authors are thankful for the financial supports from the National Natural Science Foundation of China (Grant nos. 20371010 and 20671017) and the Specialized Research Fund for the Doctoral Program of Higher Education.

References

[1] (a) R. Neumann, Prog. Inorg. Chem. 47 (1998) 317;
(b) A.M. Khenkin, L. Weiner, Y. Wang, R. Neumann, J. Am. Chem. Soc. 123 (2001) 8531;
(c) N.M. Okun, M. Travis, K.I. Hardcastle, C.L. Hill, Inorg. Chem. 42 (2003) 6610;
(d) S.S. Stahl, Angew. Chem. Int. Ed. 43 (2004) 3400.
[2] (a) J.T. Rhule, C.L. Hill, Z. Zheng, R.F. Schinazi, Top. Biol. Inorg. Chem. 2 (1999) 117;
(b) X.H. Wang, J.F. Liu, J.X. Li, Y. Yang, J.T. Liu, B. Li, M.T. Pope, J. Inorg. Biochem. 94 (2003) 279.
[3] (a) M. Clemente-León, E. Coronado, P. Delhaes, C.J. Gómez-García, C. Mingolaud, Adv. Mater. 13 (2001) 574;
(b) J.M. Clemente-Juan, E. Coronado, A. Forment-Aliaga, J.R. Galán-Mascarós, C. Giménez-Sáiz, C.J. Gómez-García, Inorg. Chem. 43 (2004) 2689;
(c) A. Forment-Aliaga, E. Coronado, M. Feliz, A. Gaita-Ariño, R. Llusar, F.M. Romero, Inorg. Chem. 43 (2004) 8019;
(d) U. Kortz, F. Hussain, M. Reicke, Angew. Chem. Int. Ed. 44 (2005) 2.
[4] (a) P. Gómez-Romero, N. Casañ-Pastor, J. Phys. Chem. 100 (1996) 12448;
(b) T. Yamase, P.V. Prokop, Angew. Chem. Int. Ed. 41 (2002) 466;
(c) T. Ruether, V.M. Hultgren, B.P. Timko, A.M. Bond, W.R. Jackson, A.G. Wedd, J. Am. Chem. Soc. 125 (2003) 10133.
[5] (a) A. Dolbecq, P. Mialane, L. Lisnard, J. Marrot, F. Sécheresse, Chem. Eur. J. 9 (2003) 914;
(b) L. Lisnard, A. Dolbecq, P. Mialane, J. Marrot, F. Sécheresse, Inorg. Chim.Acta. 357 (2004) 845;
(c) C. Dablemont, A. Proust, R. Thouvenot, C. Afonso, F. Fournier, J.C. Tabet, Inorg. Chem. 43 (2004) 3514;
(d) T. Soumahoro, E. Burkholder, W. Ouellette, J. Zubieta, Inorg. Chim. Acta. 358 (2005) 606.
[6] R. Santiago, V. Pablo, M.G.Z. Juan, L. Luis, S.F. Leire, I.B. Javier, Inorg. Chem. 44 (2005) 9731.
[7] L. Lisnard, A. Dolbecq, P. Mialane, J. Marrot, E. Codjovi, F. Sécheresse, Dalton Trans. (2005) 3913.
[8] (a) O. Kahn, Molecular Magnetism, VCH, New York, 1993;
(b) R.L. Carlin, Magnetochemistry, Spinger, Berlin, 1986.
[9] M. Sadakane, E. Steckhan, Chem. Rev. 98 (1998) 219.
[10] S. Nellutla, J.V. Tol, N.S. Dalal, L.H. Bi, U. Kortz, B. Keita, L. Nadjo, G.A. Khitrov, A.G. Marshall, Inorg. Chem. 44 (2005) 9795.
[11] S. Himeno, I. Kitazumi, Inorg. Chim. Acta. 355 (2003) 81.
[12] (a) M. Rajesh, M. Pavan, Polyhedron 17 (1998) 2607;
(b) A.T. Konstantin, O. Dermot, Inorg. Chim. 42 (2003) 1919.

[13] O. Kahn, Molecular Magnetism, VCH, Weinheim, 1993, p. 114.
[14] G.M. Sheldrick, *SHELX-TL*, version 6.12; University of Göttingen, Bruker AXS Inc.: Madison, WI, 1998.
[15] M. Sadakane, E. Steckhan, Chem. Rev. 98 (1998) 219.
[16] C. Wang, S. Zheng, G. Yang, Inorg. Chem. 46 (2007) 616.
[17] S.V. Krivovichev, P.C. Burns, Solid State Sciences 5 (2003) 373.
[18] L.H. Fan, L. Xu, G.G. Gao, F.Y. Li, Inorg. Chem. Commun. 9 (2006) 1308.